IEEE Access
Multidisciplinary | Rapid Review | Open Access Journal

Received July 23, 2019, accepted August 1, 2019, date of publication August 6, 2019, date of current version August 20, 2019.

Digital Object Identifier 10.1109/ACCESS.2019.2933427

Full-Duplex Femto Base-Station With Antenna Selection: Experimental Validation

NIDAL ZARIFEH, (Member, IEEE), YAMEN ZANTAH, (Student Member, IEEE), YUAN GAO, AND THOMAS KAISER, (Senior Member, IEEE)

Institute of Digital Signal Processing, University of Duisburg–Essen, 47057 Duisburg, Germany

Corresponding author: Nidal Zarifeh (nidal.zarifeh@uni-due.de)

This work was supported by the Open Access Publication Fund of the University of Duisburg-Essen.

ABSTRACT Full-Duplex (FD) is an emerging technology that allows the communication device to use the same frequency to simultaneously transmit and receive. The cancellation of the high power Self-Interference (SI) is the main challenge in FD systems. Hybrid SI mitigation and cancellation schemes in propagation, analog, and digital domains, have to be used in order to mitigate the SI. Antenna selection (AS) can be employed to select the best antenna, or set of antennas, that guarantees jointly the maximization of the desired signal, and the minimization of SI. In this paper, we aim to experimentally enable FD transmission in an indoor femto base-station (BS) with antenna selection. Receive antenna selection is combined with cross-polarization and antennas conditional placement in order to achieve the required SI cancellation. Half-duplex (HD) Uplink (UL) user-equipments (UE) are used to measure the effect of downlink (DL) SI on the UL reception at the FD BS receiver. Different scenarios are experimented in the testbed such as, changing the number of antennas, the type of isolation (vertical/horizontal), and the type of antennas (Omnidirectional/directional). Three AS criteria are used, and the performance of the system is evaluated in terms of bit-error-rate, sum-rate, residual SI, and FD/HD sum-rate enhancement ratio. The measurement results show that the proposed hybrid solution is feasible to enable FD transmission in the considered scenario.

INDEX TERMS Antenna selection, femtocell, full-duplex, OFDM, self-interference.

I. INTRODUCTION

Full-Duplex (FD) technology has emerged to be an attractive solution for the increasing demand for communication high rates. 5G and other future wireless systems promise the user to provide developed and new services that require a significant increase in data rates and a lower latency despite the limited wireless spectrum resources. Traditional approaches for increasing spectral efficiency, like Multiple Input Multiple Output (MIMO), and Adaptive Coding and Modulation (ACM) have almost reached their maximum limits. Thus, In-Band Full-Duplex (IBFD) -shortly known as FD- carries the opportunity to double the overall spectral efficiency of the wireless system on top of all the traditional enhancement technologies. On the contrary of previous duplex schemes, like Frequency Division Duplex (FDD) and Time Division Duplex (TDD), FD technology allows the wireless system to transmit and receive in the same frequency and at the same time.

The associate editor coordinating the review of this manuscript and approving it for publication was Zeeshan Kaleem.

Besides such important potential, FD has many other benefits such as ensuring reliability and flexibility in cognitive radio networks that implicate dynamic spectrum allocation, either by in-band full-duplex or partially band-overlap FDD. This ensures a cheaper unpaired spectrum, which is traditionally allocated for TDD operation, and also it simplifies spectrum management. Moreover, full-duplex technology enables the reuse of radio resources for access and backhaul, especially in 5G small cells [1]. In addition, full-duplex can be a potential solution for other wireless problems such as excessive latency in delay-sensitive applications and in multi-hop networks, hidden terminals, congestion, and collision.

Self-Interference (SI), which is the transmitted signal impairing the receiver's circuitry within the same transceiver, is the main obstacle against the utilization of FD technology in wireless communication systems. Since the useful signals from other nodes have low power, due to path loss and other impairment, the undesired SI signal, which is 100 dB or higher, will have a significant negative effect on receiving the useful signal. Therefore, it is necessary to mitigate

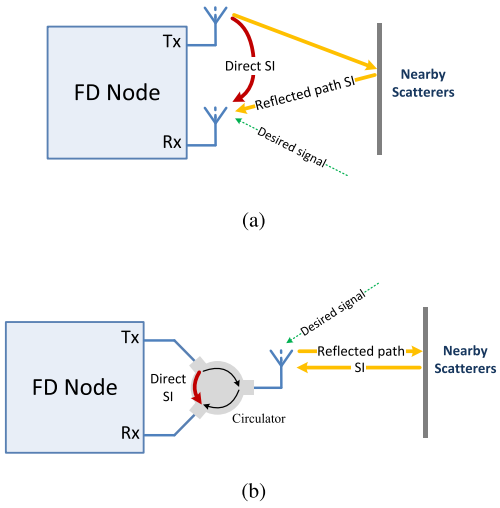

FIGURE 1. An illustration of FD node with Self-Interference (a) Separated antennas (b) Shared antenna.

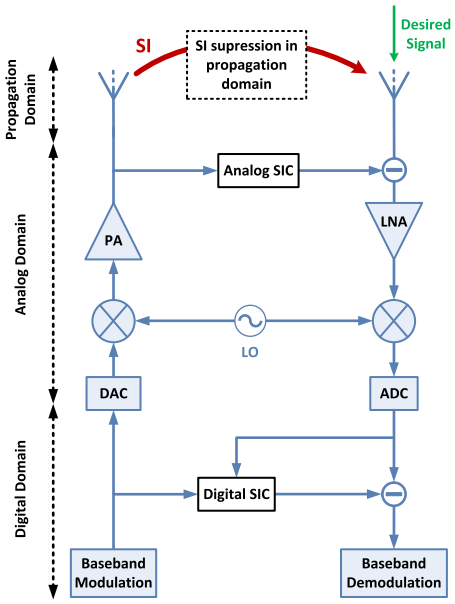

FIGURE 2. An example of an FD system with a hybrid SIC solution.

the SI signal in order to get the most out of the technical potentials that FD communication is offering. Fig. 1 illustrates the resulting SI components in an FD node with two possible setups: separated antennas, and a shared antenna with a circulator. Simply subtracting the SI signal from the overall received signal is not a valid solution for suppressing the SI. After consecutive stages of analog processing, hardware imperfections, and SI propagation channel, the SI signal is no longer fully known by the receiver. Therefore, advanced techniques of self-interference cancellation (SIC) have to be implemented to meet the expected cancellation requirements.

A. SELF-INTERFERENCE CANCELLATION

Self-interference cancellation techniques can be classified into passive SI suppression techniques, and active SI cancellation techniques [2].

Passive SI suppression techniques are employed in the propagation domain, by setting up the transmit and receive antennas with an appropriate design, in order to suppress the SI signal power before it enters the receiver. The passive suppression is demonstrated in the FD mutual antenna transceiver architecture through the isolating RF circulator, where it achieves between (15-30 dB) of suppression [2]. Passive suppression in the separate antenna architecture can be achieved by implementing cross-polarization [3]–[7], directional isolation [4]–[6], antenna conditional placement [7]–[13], or absorptive/reflective shielding [5], [9], [11]. The suppression efficiency of each of these mechanisms depends on the physical restrictions of the system. For example, the shielding mechanism is not suitable for cellular applications as it has a shadowing effect on the cell coverage; meanwhile, it would be a useful solution for FD relaying (FDR) with a directional isolation [15], [16].

Active SIC techniques, on the other hand, use a pre-processed copy of the SI signal to be subtracted from the overall received signal. We can differentiate between three active SIC classes according to the domain in which the SI signal is being mitigated:

- Pure analog processing, where both the replication of the transmitted signal and the subtraction of SI are done in the analog domain. The replication can be achieved by balanced-unbalanced circuit (Balun) [14], or a power splitter [17], [18], then the processing and the subtraction are performed using a noise-cancellation active chip such as Quellan QHx220 [12], [14], [19]. Another method is to design a printed circuit board (PCB) with several delay microstrip lines [20]; each one has a different length and is connected to a tunable attenuator to overcome the fixed delay problem in the Quellan active chip. Such techniques can achieve about 25 dB of isolation in average.
- In pure digital cancellation, the proposed schemes are based on the traditional approaches of external interference cancellation, but with customized algorithms for self-interference [12], [14], [17], [18], [20]. These schemes can provide about 25-35 dB of SIC.
- In analog/digital SIC techniques [8], [21], [22], an auxiliary transmitter is used. A copy of the transmitted samples is digitally predistorted and converted to the analog domain, then fed to the receiver in order to be subtracted from the total received signal. A similar approach can be implemented with an auxiliary receiver. In these schemes, an additional converter, digital-to-analog converter (DAC) or analog-to-digital converter (ADC), is required.

In general, an accumulative solution is required in a full-duplex Single-Input-Single-Output (SISO) system to achieve the required SIC. Fig. 2 shows a hybrid solution with a combination of the three domains techniques.

B. MULTI-ANTENNA FULL-DUPLEX SYSTEM

In the case of Multiple-Input-Multiple-Output (MIMO), the main challenge is the scalability of the SIC solution. Some works have been done with auxiliary chains as in [6] and [23], or with complicated antennas conditional placement for narrowband systems [7], whereas the authors in [24] and [25] are proposing a decoupling network as a SIC technique in the multi-antenna system. In all these works, the number of antennas is still limited to 2x2 due to the complexity of the proposed methods. Recently, beam-forming with massive MIMO is considered in many papers like [26]–[28]. The work in [4] is using dual-polarized reflect-arrays with spatial isolation to mitigate the SI. Generally, besides scalability, all multi-antenna SIC techniques still need further development and face a lot of challenges. First, the length of the pilot, which is used for SI channels estimation, is proportional to the number of antennas; hence, the accuracy of the channel estimation is limited by the coherence time and the noise correlation for long pilot sequences. Second, the effect of different types of hardware impairment on SIC performance becomes more pronounced and has to be analyzed and calibrated for the multi-antenna system with several transmitter and receiver chains. Finally and above all, the cost efficiency and the feasibility of FD realization for the aforementioned multi-antenna techniques are still a matter of question.

Antenna Selection (AS) cancellation is a simple cost-efficient technique for multi-antenna FD systems. Rather than RF elements, antennas are inexpensive. In many application scenarios, the additional hardware and the high complexity can be avoided with AS where only some RF switches are needed instead of multi-transceiver chains. This forms a motivation to use AS as an alternative SIC multi-antenna technique to reduce hardware costs and complexity dramatically. FD AS does not rely on linear SI subtraction; instead, it selects the best pair of forward/SI channels that guarantees the maximum possible rate in the environment. Such approach minimizes the effect of hardware impairment and nonlinearities on SIC performance. The use of narrowband AS in FD was adopted in [29]–[31]. The works in [32] and [33] analyze the performance of AS theoretically and with a simple simulation of a bidirectional FD multi-antenna system. In [34], a theoretical analysis is done to use AS FD in back-hauling of multiple small cell network. In wideband systems, we, in [3], proposed a practical method of wideband AS to enable full-duplex in an indoor femto base-station (femto-BS) that operates with Long-Term-Evolution (LTE) system. Similar work is done in [35] with distributed antenna system (DAS) in order to enhance the channel diversity. In both papers, we used the ray-tracing method to simulate the propagation channels.

C. CONTRIBUTIONS OF THIS PAPER

This paper is a hardware validation of our previous work in [3]. We aim to experimentally enable the FD transmission in an indoor wideband femto-BS with antenna selection. Receive antenna selection is combined with cross-polarization and antennas conditional placement in order to achieve the required SIC. Half-duplex (HD) uplink user-equipments (UE) are used to measure the effect of downlink (DL) SI on the uplink (UL) reception at the FD BS. In the proposed scenario, UEs operate in HD TDD mode as in [36]. At a certain time, part of them are acting as UL users, and the rest are receiving the DL signal. Meanwhile, the BS is working in FD mode, so it can simultaneously transmit its signal to the specific DL users and receive the signals from UL users. Another deployment scenario can be represented with the same setup, where all the users are transmitting UL signals, and the FD BS receives them and simultaneously transmits the backhaul signal to the core network in the same frequency band.

Different cases are experimented in the testbed, such as changing the number of antennas, the type of isolation (vertical/horizontal), and the type of antennas (Omnidirectional/directional). Three AS criteria are used, 1) MSNR: maximization of SNR without considering the SI channels. 2) MSSINR: maximization of SSINR, where SI channels are estimated. 3) MCGR: maximization of channel gain ratio, as will be explained later. The performance of the system is evaluated by bit-error-rate (BER), sum-rate, residual SI (RSI), and FD/HD sum-rate enhancement ratio.

After this introduction, the system model is shown in section II. The antenna selection criteria are presented in section III. Section IV explains the setup in detail: the hardware structure, the signal processing, the setup flowcharts, and the measurement environment. Section V shows the measurement results for different experiment scenarios of the FD testbed. Finally, the conclusion and future work are drawn in section VI.

II. SYSTEM MODEL

A. SIC REQUIREMENTS

As mentioned earlier, the SI signal can be cancelled accumulatively in the propagation domain, in the analog domain, and in the digital domain. None of these domains unaided can achieve the required SI cancellation; thus hybrid solutions are proposed in the literature. The main purpose of SI signal cancellation in propagation and analog domains is to prevent the saturation of the receiver's ADC. This is done by mitigating the SI signal before the low-noise amplifier (LNA) in the receiver's RF chain to reach the dynamic range of the ADC [2].

To be able to determine the requirements of SIC analytically, we must first understand the dependencies of the FD BS transceiver specifications and the attainable amount of SIC [2], which are shown in Fig. 3.

In this figure, P_{UL} and P_R are the uplink transmitted and received power of the desired signal from the remote node. P_{DL} and P_{SI} are the DL transmitted power and the SI power after the SI channel path loss. P_{ADC} is the SI signal at the input of the receiver's ADC after SIC in the analog and/or propagation domains SIC_A. Meanwhile, P_{RSI} is the residual SI power after the achievable SIC in the digital domain SIC_D.

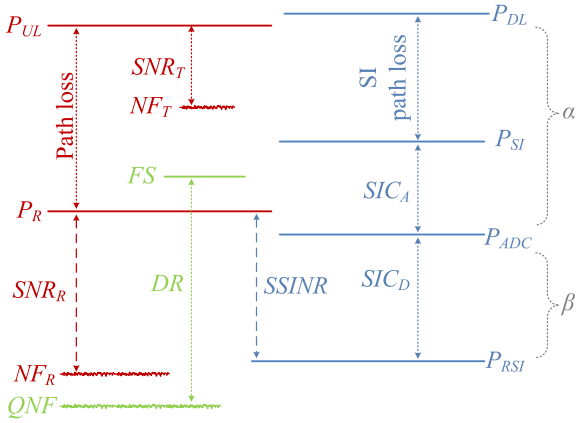

FIGURE 3. Power levels dependencies in a full-duplex BS transceiver.

The ADC specifications DR, QNF, and FS are the dynamic range, the quantization noise floor, and the full-scale level of the converter. SNR_T, NF_T and SNR_R, NF_R are the Signal-to-Noise Ratio and the noise floor at the transmitter, and at the receiver respectively.

The Signal to Self-Interference plus Noise Ratio $SSINR$ is defined as:

$$SSINR\,[dB] = P_R\,[dBm] - P_{RSI}\,[dBm]. \tag{1}$$

As long as the residual SI after the total SIC is higher than the receiver's noise floor, and correspondingly $SSINR$ is lower than SNR_R, the FD system performance will be degraded [2].

For example, if the receiver's noise floor of the FD BS is −105 dBm, and the maximum DL transmit power is 20 dBm, this entails a 125 dB of SIC -including SI path loss- in order to completely suppress the SI signal. If the accomplished SIC was not enough to reach the receiver's noise floor, the receiver would be impaired by the residual SI signal, and consequently, the system performance would be degraded. However, in a femtocell indoor environment, the requirements are slightly looser due to the low-power DL transmitted signal [37], and the less path loss of the UL transmission in such environment. Consequently, the required SI cancellation in the indoor femto BS is not as much as high as in an outdoor BS. A numerical analysis will be shown within the measurement results in this study case.

B. SELF-INTERFERENCE MODEL

In general, the SI signal is composed of the direct SI signal, and the reflections of this signal, whether they were internal reflections resulting from the form factor of the transceiver, or external reflections from the surrounding environment. However, the internal reflections are constant, because they are dependent on the transceiver form factor. The external reflections vary, on the other hand, in accordance with the surrounding environment. The power-delay-profile of the total self-interference channel is given by [38]:

$$PDP(t,\tau) = \gamma_d \delta(t,\tau_d) + \gamma_i \delta(t,\tau_i) + \sum_{p=2}^{P} \gamma_p \delta(t,\tau_p), \tag{2}$$

where γ_d, γ_i and γ_p are the power of the direct SI signal, the power of the internal reflection and the power of the p_{th} external reflection path respectively. τ_d, τ_i and τ_p are the corresponding delays. P is the total number of backscattered SI paths.

C. FULL-DUPLEX ANTENNA SELECTION SYSTEM

Along with the significant performance improvements MIMO technology offers, comes a considerable limiting factor represented by the resulting complexity due to using a dedicated RF chain for each employed antenna in conventional MIMO systems. Consequently, this would highly increase the implementation costs which escalate along with the number of employed antennas [39].

AS technique provides the possibility to reduce the accompanying costs while maintaining many of the advantages that MIMO systems offer, by using a limited number of RF chains and selecting a subset of antennas from the total available antennas. This way, the number of RF chains will be reduced to the number of the selected antennas and the implementation costs of the MIMO system will be reduced as well. The best set of antennas to be selected is determined by deploying a specific antenna selection criterion. AS can be deployed at the receiver side and/or at the transmitter side as well, with the condition that the Channel State Information (CSI) for all MIMO channels, must be known at the receiver and/or at the transmitter side respectively [40]. This condition can be met by training the MIMO channels through using pilot signals, in order to be able to estimate the channel at the receiver side, and to feedback the estimated CSI to the transmitter side in case of AS implementation at the transmitter side.

Since the essential objective of this work is the evaluation of the AS performance in mitigating the SI in an FD BS, for simplicity, we will consider only two UL single-antenna users in different locations ($U = 2$). It is clear that the number of users has a limited effect on SI mitigation performance. Further work can be done to evaluate the DL reception at different DL users, and to analyze the inter-user interference from UL users to DL users.

The FD system model is denoted in Fig. 4. We consider a femto-BS with N_r receive antennas, and a single transmit antenna that transmits the DL signal ($N_t = 1$). In HD system, and for each user the UL signal is given by the following linear model [41]:

$$y = \sqrt{E_x}\, H\, x + w, \tag{3}$$

where x is the transmitted symbol from the UL user, H is the $N_r \times 1$ channel vector, E_x is the transmission power and w is the Additive White Gaussian Noise (AWGN) following the complex Gaussian distribution with zero mean and $\sigma^2 I_{N_r}$ covariance matrix. σ^2 is the noise covariance and I_{N_r} is the

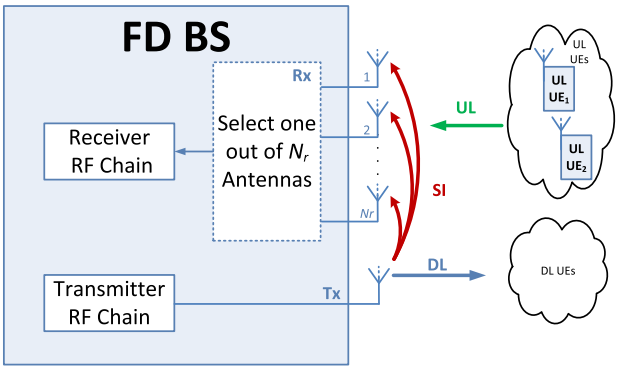

FIGURE 4. FD AS system model.

$N_r \times N_r$ identity matrix. Then the SNR is given by $\rho = E_x/\sigma^2$.

When AS technique is implemented at the receiver side in the BS, with the assumption of complete knowledge of the CSI in the receiver, one antenna is selected out of the N_r receive antennas of the BS. The signal model of the received signal using the selected receive antenna is:

$$y_s = \sqrt{E_x}\, h_s\, x_s + w_s, \tag{4}$$

where h_s is the channel response of the selected antenna, and w_s is the AWGN.

The FD system is assumed to be applied in an indoor environment, consequently, the UL signal and the SI signal experience multipath propagations.

The impulse response of the channel between the UE's transmit antenna and one of the N_r receive antennas is given by the following model [3]:

$$CIR(t,\tau) = \sum_{p=1}^{P(t)} \alpha_p(t)\, e^{-j\varphi_p(t)} \delta(\tau - \tau_p(t)), \tag{5}$$

where τ_p, α_p and φ_p are the delay, the attenuation, and the phase shift of the pth path.

The frequency domain response is obtained by applying Fourier transform to the impulse response as:

$$H(f) = \int_{-\infty}^{+\infty} CIR(\tau)\, \mathrm{e}^{-2\pi f \tau}\, d\tau. \tag{6}$$

Similar to LTE, we consider Orthogonal frequency-division multiplexing (OFDM) waveform implementation. OFDM is used to overcome the Inter-Symbol Interference (ISI), which is a result of the multi-path propagations.

The transmit symbol vector in the frequency domain is of size $N_u \times 1$, where N_u is the number of used OFDM subcarriers. After receiving the transmitted signal using all the N_r receive antennas, and estimating propagation channels, the received symbol vector in the frequency domain at the receiver baseband is given for $N_r \cdot N_u \times N_u$ by the frequency domain channel matrix:

$$H = \begin{bmatrix} H(0) & \cdots & 0 \\ \vdots & \ddots & \vdots \\ 0 & \cdots & H(N_u - 1) \end{bmatrix} \tag{7}$$

where each diagonal element $H(k)$ represents the $1 \times N_r$ channel vector for the k_{th} subcarrier:

$$H(k) = \sum_{l=1}^{L-1} G(l)\, e^{-i\frac{2\pi kl}{N_u}}, \tag{8}$$

where $G(l)$ is the $N_r \times 1$ vector for the l_{th} delay of the channel impulse response.

Now we present the baseband signal model after AS implementation, the received signal from each user at the BS using the selected antenna is given by:

$$y(k) = h_{ul}(k)x_{ul}(k) + \alpha\, \beta\, h_{si}(k)x_{dl}(k) + \sum_{q=1, q\neq u}^{U} H_q(k)x_q(k) + w(k), \tag{9}$$

where $x_{ul}(k)$ is the uplink transmitted signal from the specific UL user, and $h_{ul}(k)$ is the forward uplink channel response. $h_{si}(k)$ is the SI channel response between the BS's downlink transmit antenna and the selected receive antenna. $x_{dl}(k)$ denotes the transmitted downlink signal. β is the SI digital attenuation factor, where the maximum value of β is one when no digital SIC is implemented, and α denotes the SI suppression factor in the analog and propagation domains. The summation in (9) denotes the unwanted signals from other UL users. This term may be neglected if single-carrier frequency division multiple access (SC-FDMA) is used. In LTE, SC-FDMA guarantees the orthogonality of the uplink multiplexing. $w(k)$ is the AWGN in the receiver of the BS.

III. ANTENNA SELECTION CRITERIA

In general, the optimal AS is realized by selecting the antenna, or a subset of antennas, that achieves the maximum capacity with full rank channel matrix. In real implementation, with practical approximation, the optimal AS criterion is to maximize the SNR in an HD system, or the SSINR in an FD system. In this experiment, three AS criteria are deployed.

1) MAXIMIZATION OF SIGNAL-TO-NOISE RATIO (MSNR)

In this criterion, the BS selects the antenna a_j that maximizes the received SNR as:

$$Select\ a_j = \arg\max\{\rho\}. \tag{10}$$

ρ is the mean SNR, and it is the given by:

$$\rho = \frac{S}{N}, \tag{11}$$

where S is the uplink received signal power, and N is noise power. ρ can be calculated from (9) and with neglecting the SI part. The signal power and noise power levels must be estimated independently. In the experiment, the Cyclic Prefix (CP) data in the time domain are used to estimate the noise power as in [42].

2) MAXIMIZATION OF SIGNAL-TO-SELF-INTERFERENCE-PLUS-NOISE RATIO (MSSINR)

In [3], optimal receive AS criterion is proposed and investigated for the purpose of SI mitigation in the BS of a wideband FD system. In this criterion, the BS selects the antenna a_j with the maximum achieved SSINR:

$$Select\ a_j = \arg\max\{\Gamma\}. \tag{12}$$

Γ is the mean SSINR, and it is given by:

$$\Gamma = \frac{S}{N + SI}, \tag{13}$$

where S is the desired forward received signal power, N is the noise power, and SI is the power of the undesired self-interference signal. Γ can be calculated from (9).

3) MAXIMIZATION OF CHANNEL GAIN RATIO (MCGR)

With this criterion, the selected receive antenna is the one that achieves the maximum ratio Π between the forward channel gain and SI channel gain according to:

$$Select\ a_j = \arg\max\{\Pi\}. \tag{14}$$

Π is the CGR, and it is given by:

$$\Pi = \frac{\|h_{ul}\|^2}{\|h_{si}\|^2}, \tag{15}$$

where the channels responses are estimated during the channel training phase as will be explained later.

For multi-user in the UL, the three criteria are extended to maximize the sum value of all UL users. Then the MSNR criterion complexity is given by $O(N_u \times U \times N_r^2)$, meanwhile it is $O(N_u \times U \times N_r^2 \times N_t)$ for MSSINR, and $O(N_u \times U \times N_r \times N_t)$ for MCGR criterion.

IV. THE SETUP

A. HARDWARE STRUCTURE

Fig. 5 demonstrates the block diagram of the testbed setup, whereas Fig. 6 shows the implemented testbed in the lab. The setup consists of the following equipment:

1) **Controlling PC:** with MATLAB running on it, where the following tasks are done:
   - Generation of the transmit data in MATLAB
   - Digital signal processing of the transmit and receive data
   - Applying the proposed antenna selection criteria according to the adopted scenario
   - Sending control commands to the employed equipment
2) **Arbitrary wave generator (AWG):** where the digital transmit data are converted to an analog wideband RF signal and prepared to be sent over the air via the transmit antennas.
3) **Digital signal analyzer (DSA):** where the analog received RF signals are down-converted, digitized, and transferred to the PC for further processing in MATLAB.
4) **Arduino platform:** which is responsible for controlling the RF switch for selecting the receive antennas. The Arduino platform receives its control commands from MATLAB.

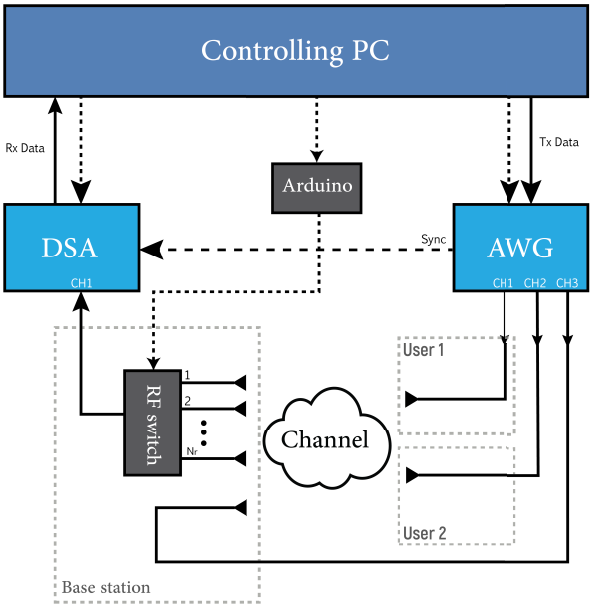

FIGURE 5. Block diagram of the full-duplex antenna selection testbed.

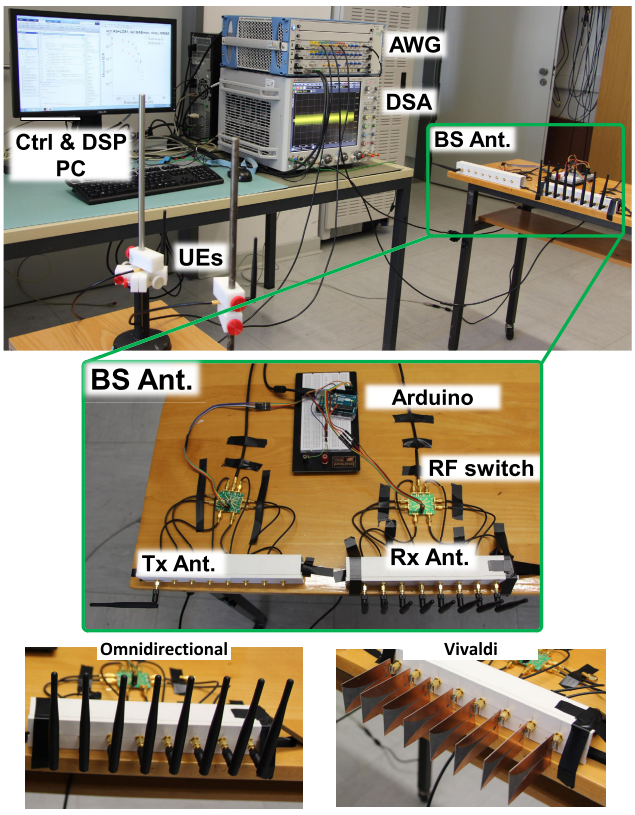

FIGURE 6. Full-duplex antenna selection testbed.

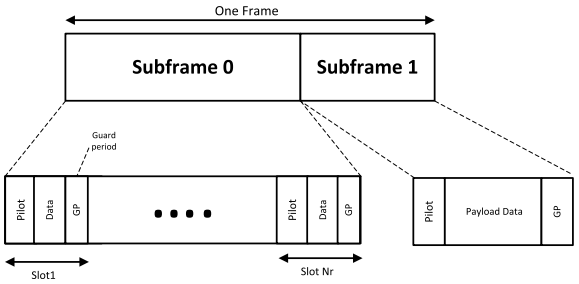

FIGURE 7. HD Frame structure.

5) **RF switch:** the RF switch has three control pins connected to Arduino platform, which correspond to eight switch ports, each port is connected to a single receive antenna.

B. SIGNAL STRUCTURE AND FLOWCHARTS

1) FRAME DESIGN

In order to determine which is the best receive antenna by deploying the antenna selection criterion, channel training must be initially done. This order is manifested in the frame design in the testbed for the HD and the FD scenarios. In the HD scenario, each frame is composed of two subframes, subframe 0 ($SF0$) and subframe 1 ($SF1$). $SF0$ is dedicated essentially for forward channels training, that is why it is composed of N_r identical slots, where N_r is the number of the BS's receive antennas. Each slot contains:

- One pilot OFDM symbol: to train one of the N_r receive antennas.
- Payload data OFDM symbols: which are used to calculate the BER of the corresponding channel after demodulation.
- Guard period: the RF switching between the antennas is done in this period.

$SF1$ is essentially dedicated for transmitting the actual payload data. After the AS criterion is deployed, and the best antenna is determined, $SF1$ is transmitted and then received using the selected antenna. $SF1$ consists of Payload data OFDM symbols and only one pilot OFDM symbol.

Fig. 7 shows the frame structure, as in [41], for the half-duplex system, where there is no downlink transmission.

In the full-duplex scenario, the channel training stage must be considered for the uplink forward channels, as well as for the SI channels, and there will be simultaneous uplink and downlink transmissions after selecting the antenna. Therefore the frame structure must be modified for the FD scenario. Fig. 8 shows the extended frame structure for the FD scenario. The uplink subframe 0 ($SF0_{UL}$) is dedicated to forward channels' training; meanwhile, the SI calibration subframe 0 ($SF0_{Cal}$) is dedicated to SI channels' training. Where $SF1_{UL}$ and $SF1_{DL}$ in the FD scenario are the uplink subframe 1 and the downlink subframe 1 respectively, which are dedicated for the actual uplink payload data transmission and the actual downlink transmission respectively. $SF1_{UL}$ and $SF1_{DL}$ have the same structure as $SF1$ in the HD scenario. It is important

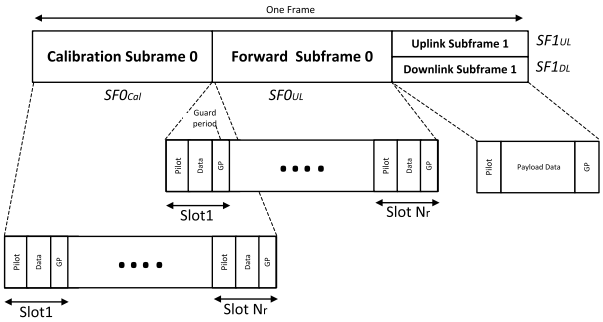

FIGURE 8. FD Frame structure, with SI channels calibration.

to notify here, that the SI channel calibration must be implemented when the experiment runs for the first time, yet it does not necessarily have to be implemented for each frame. This is because the SI channels have fewer variations than the UL forward channels, and the SI channels are more affected by the form factor of the BS, unlike the forward channels which are more subject to the surrounding environment and UEs locations. Consequently, when no SI channels calibration is required, $SF0_{Cal}$ can be omitted from the FD frame structure.

2) TRANSMISSION AND RECEPTION WORKFLOW

Fig. 9a and 9b describe the workflow of the HD AS system and the FD AS system in the experiment respectively.

In the HD scenario, the first stage is the training of the uplink forward channels. The estimation of the channel and SNR value is done for each receive antenna at the BS. After deploying the AS criterion and selecting the best receive antenna, $SF1$ is transmitted and received using the selected antenna, and further signal processing on the received data is done in MATLAB.

In the FD scenario, if the SI channels information is not obtained yet, or must be calibrated, the first stage is the training of the SI channels between the BS's downlink transmitter and each of its receive antennas. This is done by transmitting and receiving $SF0_{Cal}$, so that the SI channel matrix is estimated and the SI signal power at each receive antenna is measured. Then, sending $SF0_{UL}$ is done in order to estimate the forward uplink channel and the signal power at each receive antenna. Afterward, one of the suggested FD AS criteria is deployed, and the best receive antenna is selected. The uplink and downlink $SF1$ signals are transmitted simultaneously, and the UL reception is realized using the selected antenna.

The workflow of the forward channels' training stage is shown in Fig. 10. The first slot's data of $SF0_{UL}$ are generated and then transferred to AWG, where the data are stored and transmitted repeatedly. The RF switch is then switched during the guard period of the slot to the corresponding receive antenna. The received data are then collected by the DSA and transferred to the controlling PC to be processed in MATLAB. The cycle of switching and receiving is repeated until N_r slots data are received using the corresponding N_r receive antennas so that all the forward channels are estimated.

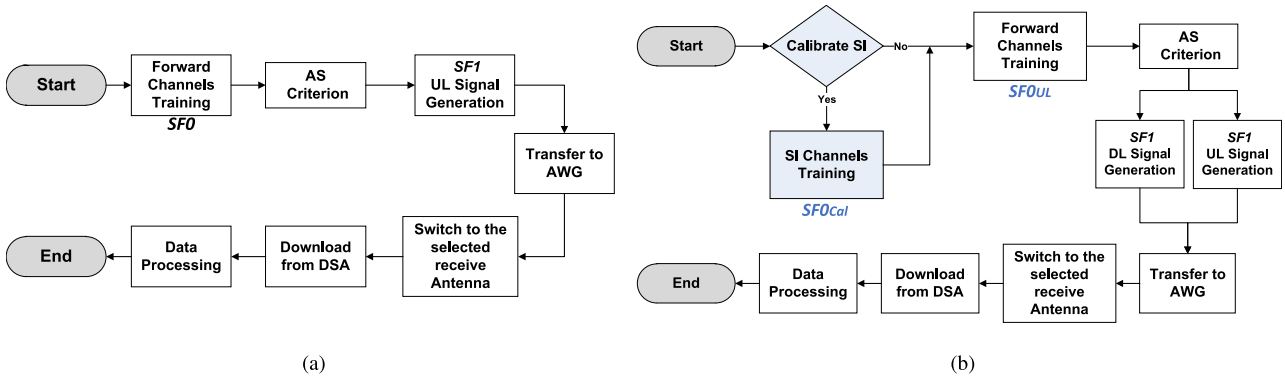

FIGURE 9. Flowchart of the experiment (a) HD (b) FD with SI channel calibration.

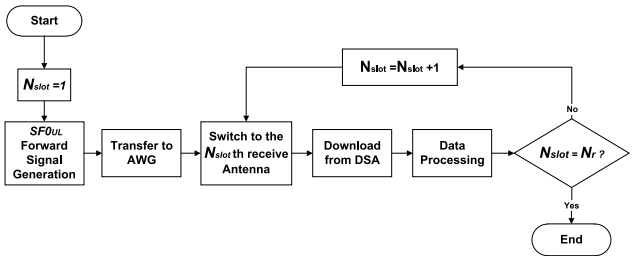

FIGURE 10. Channel estimation flowchart.

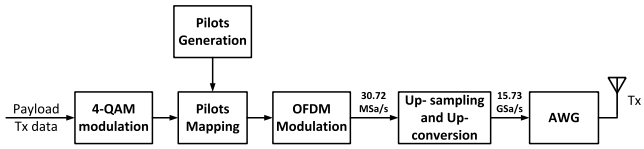

FIGURE 11. Transmission Signal Processing.

Channels training has the exact same stages, whether it is HD or FD operating scenario, and whether the uplink or the SI channels are being trained, the difference is the training subframe that is being used in the training process.

C. SIGNAL PROCESSING IN THE SETUP

The sequence of signal processing stages at the transmitter's side of the experiment is presented in Fig. 11.

The transmit payload data are digitally modulated into 4-QAM with a gray-coded signal constellation, the training pilots are generated and then mapped to the payload symbols. Afterward, the OFDM signal is digitally generated with a sampling rate of 30.72 MSa/s. The OFDM waveform parameters are presented in Table 1. The baseband signal is then up-sampled to the AWG's required sampling rate of 15.73 GSa/s, and up-converted to the carrier frequency of 5.2 GHz. The wideband OFDM signal is then transferred to the AWG to be transmitted using the transmit antenna. It must be notified here, that the signal processing stages are similar for the uplink and the downlink signals transmissions, yet the differences are, that each transmission case uses different

TABLE 1. Table of OFDM waveform parameters.

OFDM Parameter	Value
Carrier Frequency, f_c	5.2 GHz
FFT Size, N_{FFT}	2048
Subcarrier Spacing, Δ_f	15 KHz
Number of used Subcarriers, N_c	300
Bandwidth, B	4.5 MHz
Sampling Rate, f_s	30.72 MSa/s
Cyclic Prefix Duration, t_{cp}	8.33 μs
OFDM Symbol Duration, t_{symb}	75 μs
Modulation Scheme	4-QAM

transmit payload data, and is carried out by using a dedicated AWG channel.

It is worth mentioning here, that the OFDM samples in the time domain are Gaussian-like with a high peak to average power ratio (PAPR). In order to use the full dynamic range of the AWG DACs, which means increasing the average transmit power with the fixed full-scale AWG DACs, the PAPR has to be reduced before the AWG DAC. In this experiment, the PAPR reduction is performed using the conventional clipping method. The samples which exceed a threshold are clipped to the threshold values as in [43].

At the receiver's side, the wideband OFDM signals are received using one of the receive antennas and then directed to the DSA for analog to digital conversion, where the determined sampling rate for the DSA is 20 GSa/s, the wideband signal is then down-sampled with the baseband OFDM sampling rate of 30.72 MSa/s, and down-converted to the baseband frequency. Afterward, the signal is OFDM demodulated to get the training pilots and payload symbols. The training pilots are used for channel and power estimation, where the payload symbols are 4-QAM demodulated, and the resulting received bitstream is used to calculate the BER of this transmission by comparing it to the transmitted payload bitstream. Since no channel coding is implemented in the testbed, the calculated error rate here is uncoded BER.

D. THE MEASUREMENT ENVIRONMENT

In order to achieve the experiment measurements at a variation of SNR values at the receiver's side, ten output voltage

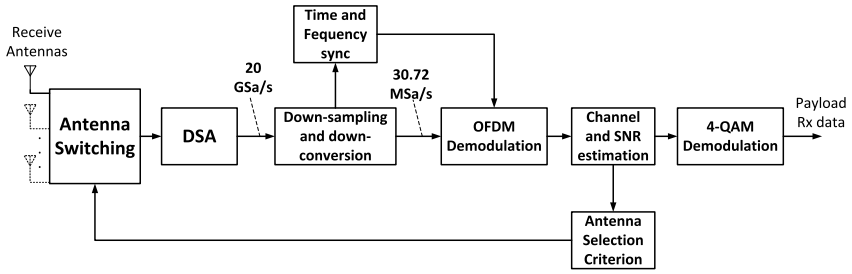

FIGURE 12. Reception Signal Processing.

TABLE 2. Measured uplink transmission power levels.

AWG's output volatge [V]	0.1	0.2	0.3	0.4	0.5	0.6	0.7	0.8	0.9	1
UL transmit power [dBm]	-19	-13.4	-10.1	-7.8	-6.1	-4.8	-3.6	-2.5	-1.6	-0.7

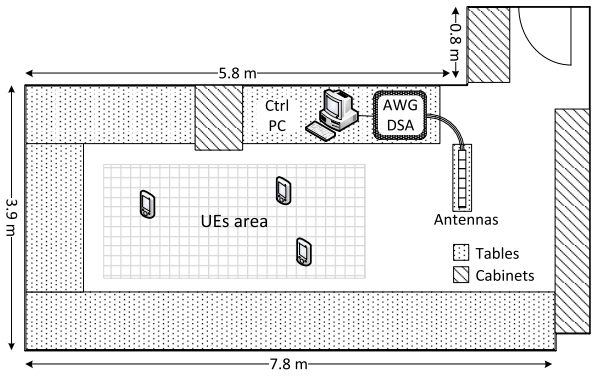

FIGURE 13. The experiment environment.

values of the AWG's output are considered for the uplink signal transmission, which corresponds to ten transmission power values as denoted in Table 2. The AWG's output level for the DL SI transmission signal is always set to the maximum possible output value of (1 [V]), which corresponds to about 0 dBm transmission power.

The UL signal transmission is conducted at different UE-BS separation distances between 1 and 4 m, and considering the line of sight communication scenario. These separation distances correspond to path loss from 45 to 60 dB. Consequently, the received power levels at the femto BS receiver are between −45 and −80 dBm. The distance between the Tx antenna and the closest Rx antenna is about 26 cm, which equals to 9 times of the half wavelength. This distance provides far-field propagation and achieves about 35 dB of SI isolation.

Figure 13 depicts the indoor environment where the experiment is performed. The multipath channels are modelled and estimated with time-domain Least Square (LS) based method as in [44].

In order to increase the accuracy of the measurement results, the experiment is repeated for at least twenty times for each transmission power value, and the average results are then considered. When the experiment operates in the presence of the SI signal in the FD scenario, the SI channels are calibrated once for every ten trials of the experiment, considering that, the SI channels have much fewer channel variations than the forward channels.

V. THE MEASUREMENT RESULTS

A. HD ANTENNA SELECTION

The measurement results of the HD MSNR AS criterion are presented in Fig. 14, where we can see the BER performance with and without applying the HD AS criterion at two different UE-BS separation values (1m, 2m). It is obvious that applying HD AS criterion overcomes the case when no AS is applied (i.e., the 1 × 8 SIMO system) at both UE-BS separation distances with better BER performances. We can see as well, that a better BER performance enhancement is achieved by applying the HD AS criterion at (2m) UE-BS separation, than at (1m) separation, due to better achieved multi-path diversity at (2m) separation.

The channel capacity of the SIMO system when no antenna selection is implemented is given by:

$$C_{NoAs} = \log_2(1 + \rho_a), \tag{16}$$

where ρ_a is the average estimated SNR per receive antenna before AS in subframe 0. When the HD AS criterion is employed, the channel capacity is calculated by:

$$C_{HD_{sel}} = \log_2(1 + \rho_{sel}), \tag{17}$$

where ρ_{sel} is the estimated SNR at the selected antenna, and is calculated as in (11).

The sum-rate for the previous cases is presented in Fig. 15. We can see that the channel capacity performance for (2m) separation is better than (1m) separation as the channels in the former case have more diversity.

B. FD AS WITH THREE CRITERIA

The three criteria are used in the FD system with 8 receive antennas. The BER performance comparison is shown in Fig. 16. The three criteria achieve similar BER performances at low SNR values. This can be justified due to the high noise power, which causes considerable errors during

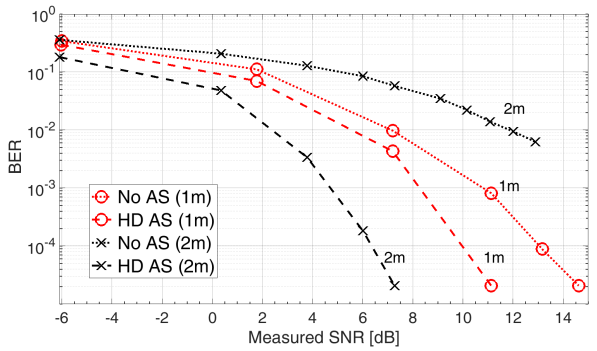

FIGURE 14. HD BER - AS with 8 antennas.

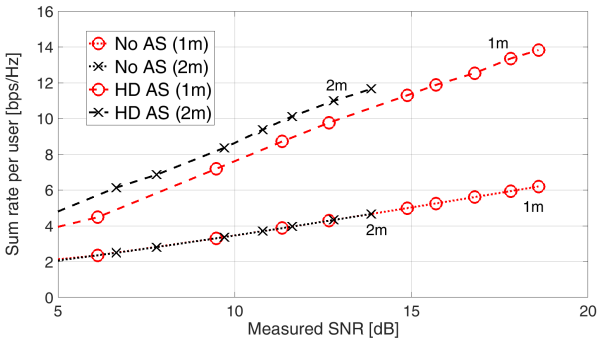

FIGURE 15. HD rate - AS with 8 antennas.

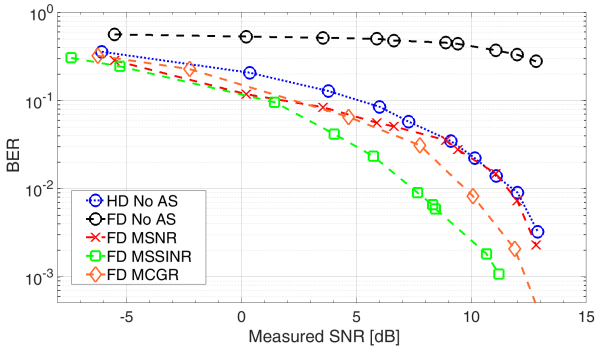

FIGURE 16. FD BER - AS with 8 antennas.

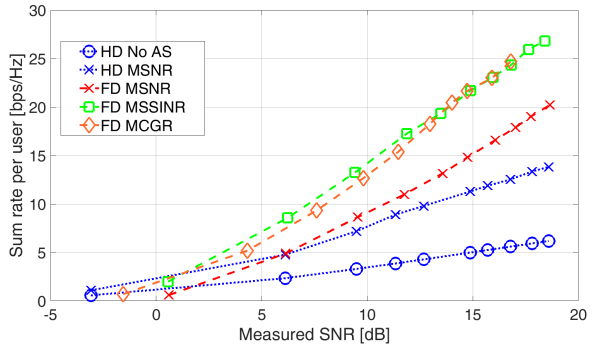

FIGURE 17. FD sum rate - AS with 8 antennas.

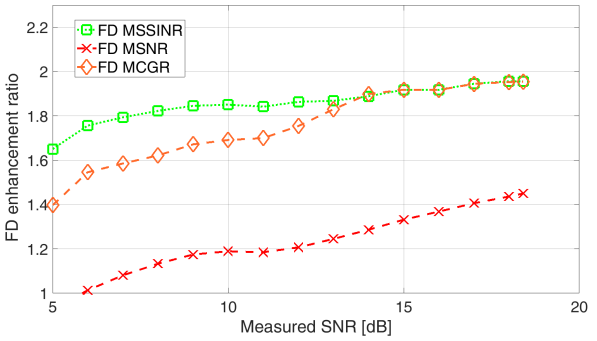

FIGURE 18. FD/HD ratio - AS with 8 antennas.

forward and SI channels estimation. Whereas at high SNR values, the MSSINR criterion overcomes the other two AS criteria. MSNR criterion performs the worst among the three criteria because it only considers the forward channel for the selection.

Fig. 17 compares the sum-rate per user performance for the three criteria. The rate can be calculated as in the HD system, except using SSINR, Γ_{sel} from (13), instead of SNR ρ_{sel}.

MSSINR achieves slightly better capacity compared to MCGR at low SNRs; meanwhile, they have the same performance when the noise power is much lower than the signal. Such observation can be also seen in Fig. 18. The figure shows the enhancement ratio of FD rate over the HD rate. At high SNRs, both MSSINR and MCGR criteria almost reach the theoretical boundary of 2. The residual SI, that can be in some measurements about 3 to 6 dB over the noise, prevents the FD system of exactly doubling the sum-rate. This is due to the channels estimation errors, nonlinearities, and the PAPR of the OFDM signal. MSNR performance is quite lower compared to the two FD criteria, achieving around 1.45 in the best case. Measurements show that SI channel path loss guarantees about 30 to 35 dB of isolation. Besides the digital SIC, which is $\beta = 20$ dB, the AS and cross-polarization provide each about 10 to 15 dB of cancellation. The amount of SIC in propagation and analog domain is $\alpha = 55$ to 65 dB. The total amount of the achieved SIC is 75 to 85 dB, making SI almost reach the devices measured noise floor which is around -80 dBm.

C. NUMBER OF ANTENNAS

We aim here to measure the effect of the number of receive antennas in the base-station. Three cases are considered $N_r \in \{2, 4, 8\}$. In order to compare the performance of the three cases fairly, the residual SI over the noise is measured before applying any digital SIC. This reflects the SI mitigation that can be achieved in the analog domain for each case.

RSI can be extracted by subtracting the maximum attainable SSINR, in case of FD, from the maximum attainable SNR of the HD system. Fig. 19 shows the measured RSI with the two AS criteria, MSSINR and MCGR. It is clear that for 8 antennas the RSI is below 25 dB, which means less complicated digital SIC is required compared to the case of 2 and 4 receive antennas.

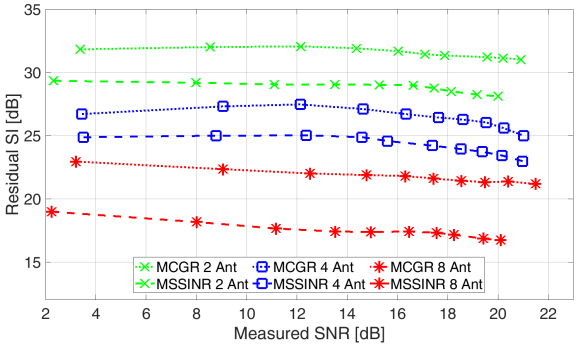

FIGURE 19. RSI in case of different number of antennas.

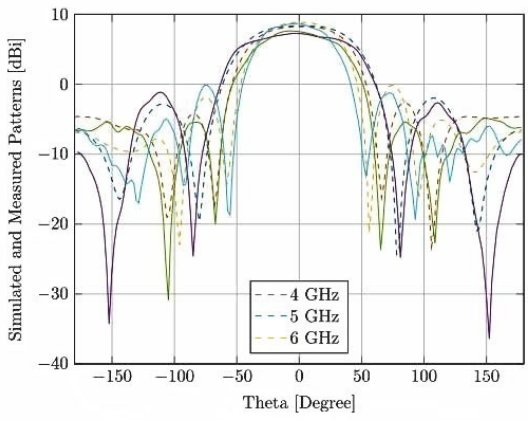

FIGURE 20. Vivaldi directional antenna pattern.

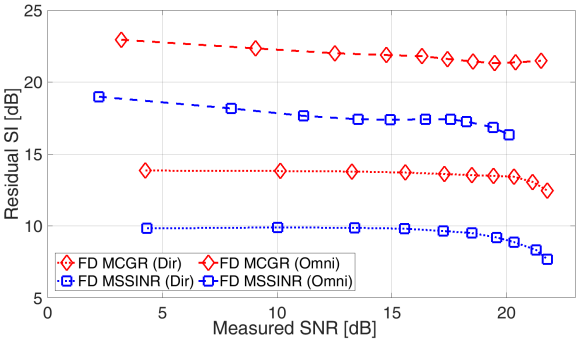

FIGURE 21. RSI with directional antennas.

Figures 22 and 23 show the performance enhancement in terms of BER and capacity.

D. DIRECTIONAL ANTENNAS

Using directional antennas in the base-station provides better SI isolation. Thus, Vivaldi antennas are used with the radiation pattern as in Fig. 20. The advantages of Vivaldi antennas are their broadband characteristics and easy manufacturing using printed circuit boards. The 3-dB beamwidth of the used antennas is about 50 degrees, this guarantees better isolation between the transmit and receive antennas in the base-station,

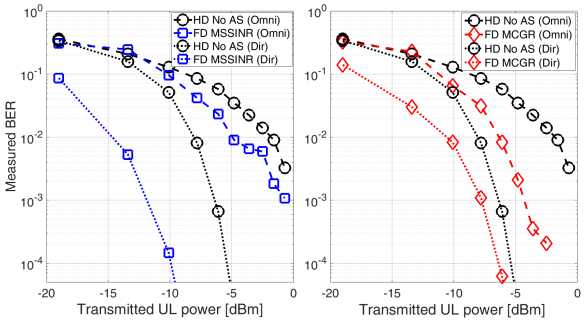

FIGURE 22. BER with directional antennas.

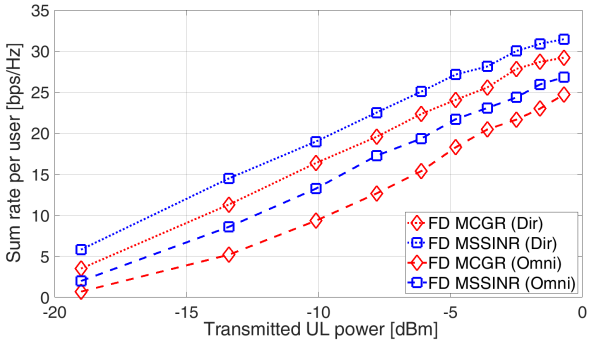

FIGURE 23. Sum rate with directional antennas.

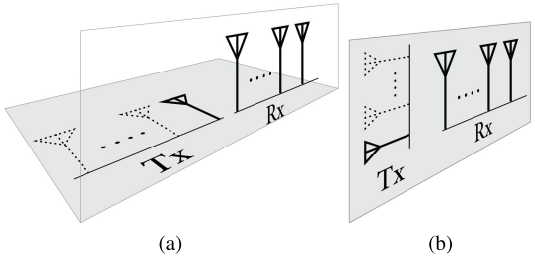

FIGURE 24. An illustration of two separation structures (a) horizontal structure (b) vertical structure.

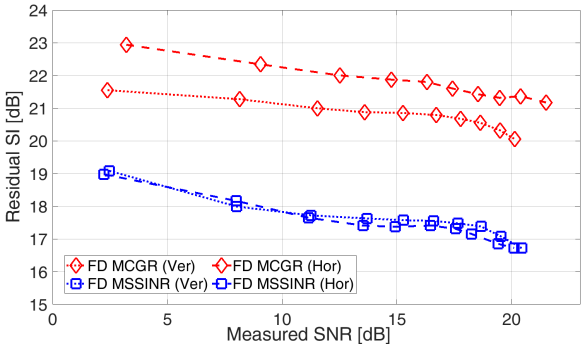

FIGURE 25. Vertical vs horizontal isolation RSI.

and therefore a better FD performance. The UEs antennas, on the other hand, remain omnidirectional in both cases, so only the BS antennas are changed. Fig. 21 shows the

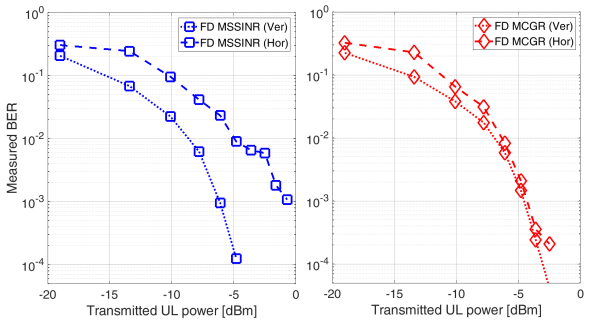

FIGURE 26. Vertical vs horizontal isolation BER.

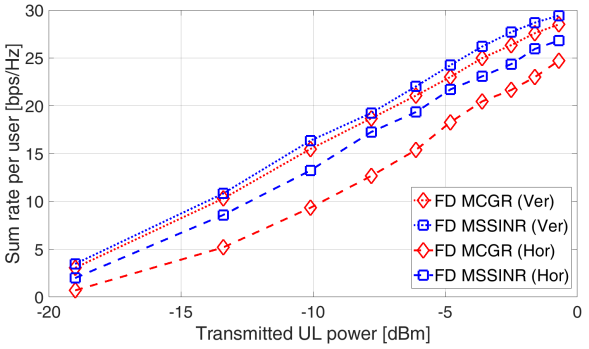

FIGURE 27. Vertical vs horizontal isolation sum rate.

residual SI in both cases and with the two AS criteria, MSSINR and MCGR. It is obvious that the RSI in the case of directional antennas is about 7 to 9 dB lower than the omnidirectional antenna. Although the benefit of using directional antennas is clear regarding SI isolation, it may cause limitations on BS coverage in some scenarios.

E. HORIZONTAL AND VERTICAL ANTENNA SEPARATION

Better isolation can be achieved by changing the type of separation between receive and transmit antennas, as shown in figure 24. By keeping the cross-polarization, and positioning the receive antennas within the axis of transmit dipole antennas, the setup can provide further SI mitigation. We can name such setup as ''vertical structure separation'' instead of the ''horizontal structure separation'' that is used in the previous measurements. However, the geometry of separation is related to the number of antennas, which has an impact on the form factor of the designed base-station.

The figures 25, 26, and 27 show the performance evaluation of the two separation types in terms of RSI, BER, and capacity.

VI. CONCLUSION

In this paper, we experimentally enabled the FD transmission in an indoor wideband femto-BS with antenna selection. Receive antenna selection is combined with cross-polarization and antennas conditional placement in order to achieve the required amount of SIC, besides conventional digital interference cancellation. Three AS criteria were used, 1) MSNR: maximization of SNR. 2) MSSINR: where SI channels are estimated and considered. 3) MCGR: maximization of channel gain ratio. The performance of the system is evaluated by uncoded bit-error-rate, sum-rate, residual SI, and FD/HD sum-rate enhancement ratio.

The hybrid SIC solution achieved about 75 to 85 dB which is acceptable for the experiment scenario of a small indoor cell. Performance comparisons were made for different cases in the testbed, like changing the number of antennas, type of isolation (vertical/horizontal), and the type of antennas (Omnidirectional/directional). Both MCGR and MSSINR show similar performance, especially in high SNR values. However, MCGR guarantees less complexity when increasing the number of antennas.

The setup focused on the base-station side, so wider analysis can be done to include the user side. For example, duplex interference (from UL users to DL users) has to be considered especially with high number of users. Also, more complex AS scenarios and algorithms can be implemented, such as transmitter antenna selection while including DL channel estimation into the AS criteria in order to increase the cell total throughput. Channel coding and channels' estimation error can be also considered to optimize the whole operation. Furthermore, the high-quality devices that were used in the experiment guaranteed minimum hardware impairment. When practical or off the shelf components are used, performance degradation is expected. This would be an interesting topic for investigation and experimentation in future works. Nevertheless, the outcome of this work could be a step further toward adopting full-duplex in 5G mobile systems and beyond.

REFERENCES

[1] S. Hong, J. Brand, J. I. Choi, M. Jain, J. Mehlman, S. Katti, and P. Levis, "Applications of self-interference cancellation in 5G and beyond," *IEEE Commun. Mag.*, vol. 52, no. 2, pp. 114–121, Feb. 2014.

[2] T. Kaiser and N. Zarifeh, "General principles and basic algorithms for full-duplex transmission," in *Signal Processing for 5G: Algorithms and Implementations*, F.-L. Luo and C. Zhang, Eds. Hoboken, NJ, USA: Wiley, 2016, ch. 16, pp. 372–401.

[3] N. Zarifeh, M. Alissa, T. Kreul, and T. Kaiser, "Enabling full-duplex in a wideband indoor base-station using low-complex antenna selection," in *Proc. Loughborough Antennas Propag. Conf. (LAPC)*, Loughborough, U.K., Nov. 2018, pp. 1–5.

[4] N. Zarifeh, M. Alissa, M. Khaliel, and T. Kaiser, "Self-interference mitigation in full-duplex base-station using dual polarized reflect-array," in *Proc. 11th German Microw. Conf. (GeMiC)*, Freiburg, Germany, Mar. 2018, pp. 180–183.

[5] E. Everett, A. Sahai, and A. Sabharwal, "Passive self-interference suppression for full-duplex infrastructure nodes," *IEEE Trans. Wireless Commun.*, vol. 13, no. 2, pp. 680–694, Feb. 2014.

[6] M. Duarte, A. Sabharwal, V. Aggarwal, R. Jana, K. K. Ramakrishnan, C. W. Rice, and N. K. Shankaranarayanan, "Design and characterization of a full-duplex multiantenna system for WiFi networks," *IEEE Trans. Veh. Technol.*, vol. 63, no. 3, pp. 1160–1177, Mar. 2014.

[7] E. Aryafar, M. A. Khojastepour, K. Sundaresan, S. Rangarajan, and M. Chiang, "MIDU: Enabling MIMO full duplex," in *Proc. 18th Annu. Int. Conf. Mobile Comput. Netw.* New York, NY, USA: ACM, Aug. 2012, pp. 257–268.

[8] M. Duarte and A. Sabharwal, "Full-duplex wireless communications using off-the-shelf radios: Feasibility and first results," in *Proc. Conf. Rec. 44th Asilomar Conf. Signals, Syst. Comput.*, Pacific Grove, CA, USA, Nov. 2010, pp. 1558–1562.

[9] C. R. Anderson, S. Krishnamoorthy, C. G. Ranson, T. J. Lemon, W. G. Newhall, T. Kummetz, and J. H. Reed, "Antenna isolation, wideband multipath propagation measurements, and interference mitigation for on-frequency repeaters," in *Proc. IEEE SoutheastCon*, Greensboro, NC, USA, Mar. 2004, pp. 110–114.

[10] M. A. Khojastepour, K. Sundaresan, S. Rangarajan, X. Zhang, and S. Barghi, "The case for antenna cancellation for scalable full-duplex wireless communications," in *Proc. 10th ACM Workshop Hot Topics Netw. (HotNets-X)*. New York, NY, USA: ACM, Nov. 2011, Art. no. 17.

[11] A. Sahai, G. Patel, and A. Sabharwal, "Pushing the limits of full-duplex: Design and real-time implementation," Jul. 2011, *arXiv:1107.0607*. [Online]. Available: https://arxiv.org/abs/1107.0607

[12] J. I. Choi, M. Jain, K. Srinivasan, P. Levis, and S. Katti, "Achieving single channel, full duplex wireless communication," in *Proc. 16th Annu. Int. Conf. Mobile Comput. Netw.* New York, NY, USA: ACM, Sep. 2010, pp. 1–12.

[13] J. I. Choi, S. Hong, M. Jain, S. Katti, P. Levis, and J. Mehlman, "Beyond full duplex wireless," in *Proc. Conf. Rec. 46th Asilomar Conf. Signals, Syst. Comput. (ASILOMAR)*, Nov. 2012, pp. 40–44.

[14] M. Jain, J. I. Choi, T. Kim, D. Bharadia, S. Seth, K. Srinivasan, P. Levis, S. Katti, and P. Sinha, "Practical, real-time, full duplex wireless," in *Proc. 17th Annu. Int. Conf. Mobile Comput. Netw.* Las Vegas, NV, USA: ACM, Sep. 2011, pp. 301–312.

[15] P. Lioliou, M. Viberg, M. Coldrey, and F. Athley, "Self-interference suppression in full-duplex MIMO relays," in *Proc. Conf. Rec. 44th Asilomar Conf. Signals, Syst. Comput.*, Pacific Grove, CA, USA, Nov. 2010, pp. 658–662.

[16] T. Riihonen, S. Werner, and R. Wichman, "Spatial loop interference suppression in full-duplex MIMO relays," in *Proc. Conf. Rec. 43rd Asilomar Conf. Signals, Syst. Comput.*, Pacific Grove, CA, USA, Nov. 2009, pp. 1508–1512.

[17] E. Ahmed and A. M. Eltawil, "All-digital self-interference cancellation technique for full-duplex systems," *IEEE Trans. Wireless Commun.*, vol. 14, no. 7, pp. 3519–3532, Jul. 2015.

[18] J. Li, H. Zhang, and M. Fan, "Digital self-interference cancellation based on independent component analysis for co-time co-frequency full-duplex communication systems," *IEEE Access*, vol. 5, pp. 10222–10231, 2017.

[19] B. Radunovic, D. Gunawardena, P. Key, A. Proutiere, N. Singh, V. Balan, and G. Dejean, "Rethinking indoor wireless mesh design: Low power, low frequency, full-duplex," in *Proc. 4th IEEE Workshop Wireless Mesh Netw.*, Boston, MA, USA, Jun. 2010, pp. 1–6.

[20] D. Bharadia, E. McMilin, and S. Katti, "Full duplex radios," in *Proc. ACM SIGCOMM Conf. SIGCOMM*. New York, NY, USA: ACM, Aug. 2013, pp. 375–386.

[21] R. Askar, T. Kaiser, B. Schubert, T. Haustein, and W. Keusgen, "Active self-interference cancellation mechanism for full-duplex wireless transceivers," in *Proc. 9th Int. Conf. Cogn. Radio Oriented Wireless Netw. Commun. (CROWNCOM)*, Oulu, Finland, Jun. 2014, pp. 539–544.

[22] R. Askar, N. Zarifeh, B. Schubert, W. Keusgen, and T. Kaiser, "I/Q imbalance calibration for higher self-interference cancellation levels in Full-Duplex wireless transceivers," in *Proc. 1st Int. Conf. 5G Ubiquitous Connectivity*, Akaslompolo, Finland, Nov. 2014, pp. 92–97.

[23] D. Lee and B.-W. Min, "2×2 MIMO in-band full-duplex radio front-end with 50 dB self-interference cancellation in 90 mHz bandwidth," in *IEEE MTT-S Int. Microw. Symp. Dig.*, Honolulu, HI, USA, Jun. 2017, pp. 670–672.

[24] R. Askar, F. Baum, W. Keusgen, and T. Haustein, "Decoupling-based self-interference cancellation in MIMO full-duplex wireless transceivers," in *Proc. IEEE Int. Conf. Commun. Workshops (ICC Workshops)*, Kansas City, MO, USA, May 2018, pp. 1–6.

[25] R. Askar, A. Hamdan, W. Keusgen, and T. Haustein, "Analysis of utilizing lossless networks for self-interference cancellation purpose," in *Proc. IEEE Wireless Commun. Netw. Conf. (WCNC)*, Barcelona, Spain, Apr. 2018, pp. 1–6.

[26] E. Everett, C. Shepard, L. Zhong, and A. Sabharwal, "SoftNull: Many-antenna full-duplex wireless via digital beamforming," *IEEE Trans. Wireless Commun.*, vol. 15, no. 12, pp. 8077–8092, Dec. 2016.

[27] R. Sultan, L. Song, K. G. Seddik, and Z. Han, "Full duplex in massive MIMO systems: Analysis and feasibility," in *Proc. IEEE Globecom Workshops (GC Wkshps)*, Washington, DC, USA, Dec. 2016, pp. 1–6.

[28] A. Shojaeifard, K.-K. Wong, M. D. Renzo, G. Zheng, K. A. Hamdi, and J. Tang, "Massive MIMO-enabled full-duplex cellular networks," *IEEE Trans. Commun.*, vol. 65, no. 11, pp. 4734–4750, Nov. 2017.

[29] M. Zhou, H. Cui, L. Song, and B. Jiao, "Transmit-receive antenna pair selection in full duplex systems," *IEEE Wireless Commun. Lett.*, vol. 3, no. 1, pp. 34–37, Feb. 2014.

[30] F. M. Maciel-Barboza, J. Sánchez-García, S. Armas-Jiménez, and L. Soriano-Equigua, "Uplink and downlink user and antenna selection for mmWave full duplex multiuser systems," in *Proc. 2nd Int. Conf. Frontiers Signal Process. (ICFSP)*, Warsaw, Poland, Oct. 2016, pp. 142–146.

[31] M. Zhou, L. Song, and Y. Li, "Joint transmit and receive antennas selection for full duplex MIMO systems," in *Proc. IEEE Global Commun. Conf.*, Austin, TX, USA, Dec. 2014, pp. 3838–3843.

[32] S. Jang, M. Ahn, H. Lee, and I. Lee, "Antenna selection schemes in bidirectional full-duplex MIMO systems," *IEEE Trans. Veh. Technol.*, vol. 65, no. 12, pp. 10097–10100, Dec. 2016.

[33] D. G. Wilson-Nunn, A. Chaaban, A. Sezgin, and M.-S. Alouini, "Antenna selection for full-duplex MIMO two-way communication systems," *IEEE Commun. Lett.*, vol. 21, no. 6, pp. 1373–1376, Jun. 2017.

[34] G. Chen, Y. Gong, P. Xiao, and R. Tafazolli, "Dual antenna selection in self-backhauling multiple small cell networks," *IEEE Commun. Lett.*, vol. 20, no. 8, pp. 1611–1614, Aug. 2016.

[35] N. Zarifeh, M. Alissa, T. Kreul, and T. Kaiser, "Antenna selection performance of distributed antenna systems in full-duplex indoor base station," in *Proc. 12th German Microw. Conf. (GeMiC)*, Stuttgart, Germany, Mar. 2019, pp. 32–35.

[36] M. Mohammadi, H. A. Suraweera, Y. Cao, I. Krikidis, and C. Tellambura, "Full-duplex radio for uplink/downlink wireless access with spatially random nodes," *IEEE Trans. Commun.*, vol. 63, no. 12, pp. 5250–5266, Dec. 2015.

[37] M. Yavuz, F. Meshkati, S. Nanda, A. Pokhariyal, N. Johnson, B. Raghothaman, and N. Richardson, "Interference management and performance analysis of UMTS/HSPA+ femtocells," *IEEE Commun. Mag.*, vol. 47, no. 9, pp. 102–109, Sep. 2009.

[38] T. Le-Ngoc and A. Masmoudi, *Full-Duplex Wireless Communications Systems Self Interference Cancellation*. Cham, Switzerland: Springer, 2018.

[39] A. Gorokhov, D. A. Gore, and A. J. Paulraj, "Receive antenna selection for MIMO spatial multiplexing: Theory and algorithms," *IEEE Trans. Signal Process.*, vol. 51, no. 11, pp. 2796–2807, Nov. 2003.

[40] A. F. Molisch and M. Z. Win, "MIMO systems with antenna selection," *IEEE Commun. Mag.*, vol. 5, no. 1, pp. 46–56, Mar. 2004.

[41] Y. Gao, "Low RF-complexity massive MIMO systems: Antenna selection and hybrid analog-digital beamforming," Ph.D. dissertation, Inst. Digit. Signal Process., Duisburg-Essen Univ., Duisburg, Germany, 2017.

[42] F.-X. Socheleau, A. Aissa-El-Bey, and S. Houcke, "Non data-aided SNR estimation of OFDM signals," *IEEE Commun. Lett.*, vol. 12, no. 11, pp. 813–815, Nov. 2008.

[43] R. O'Neill, and L. B. Lopes, "Envelope variations and spectral splatter in clipped multicarrier signals," in *Proc. 6th Int. Symp. Pers., Indoor Mobile Radio Commun.*, Toronto, ON, Canada, Sep. 1995, pp. 71–75.

[44] L. Deneire, P. Vandenameele, L. van der Perre, B. Gyselinckx, and M. Engels, "A low-complexity ML channel estimator for OFDM," *IEEE Trans. Commun.*, vol. 51, no. 2, pp. 135–140, Feb. 2003.

NIDAL ZARIFEH (S'17–M'19) received the B.Sc. degree in electronics and communication engineering from Damascus University, Syria, in 2006, the master's degree in advanced telecommunication engineering, specialized in mobile communication, jointly from Telecom Bretagne, Brest, France, and Damascus University, Syria, in 2012. He is currently pursuing the Ph.D. degree with the Institute of Digital Signal Processing, University of Duisburg–Essen, Germany, where he joined, in 2013 and works in several research projects, national and European wide, focusing on 5G mobile technologies, full-duplex, cognitive radio, and massive MIMO. He developed practical experience in GSM, UMTS, and LTE, working as a Radio Studies and Optimization Engineer in different mobile operators.

YAMEN ZANTAH (S'19) received the B.Sc. degree in electronic and communication engineering from Al-Baath University, Syria, in 2011, and the M.Sc. degree in embedded systems engineering from the University of Duisburg–Essen, in 2019. From 2012 to 2014, he was the Head of the Communication Team, SADCOP, Syria. He is currently a Research Scholar with the Institute of Digital Signal Processing, University of Duisburg–Essen. His research interests include full-duplex, massive MIMO, antenna selection, and millimeter and terahertz wave technologies.

YUAN GAO received the B.Sc. degree from the School of Information Science and Engineering, Shandong University, Jinan, China, in 2008, the M.Sc. degree from the Faculty of Electrical Engineering and Information Technology, RWTH Aachen University, Aachen, Germany, in 2011, and the Ph.D. degree from the Institute of Digital Signal Processing, University of Duisburg–Essen, Duisburg, Germany, in 2017. He is currently working on 5G NR system design including cell search and beam management. His research interests include signal processing, especially in the wireless communication systems, including cognitive radio in LTE systems, RF modeling, massive MIMO signal processing such as MIMO detection, antenna selection, and hybrid beamforming.

THOMAS KAISER (M'98–SM'04) received the Diploma degree in electrical engineering from Ruhr-University Bochum, Bochum, Germany, in 1991, and the Ph.D. (Hons.) and German Habilitation degrees in electrical engineering from Gerhard Mercator University, Duisburg, Germany, in 1995 and 2000, respectively. From 1995 to 1996, he spent a research leave with the University of Southern California, Los Angeles, CA, USA, which was grant-aided by the German Academic Exchange Service. From 2000 to 2001, he was the Head of the Department of Communication Systems, Gerhard Mercator University, Duisburg. From 2001 to 2002, he was the Head of the Department of Wireless Chips and Systems, Fraunhofer Institute of Microelectronic Circuits and Systems, Duisburg. From 2002 to 2006, he was a Co-Leader of the Smart Antenna Research Team, University of Duisburg–Essen, Duisburg. In 2005, he joined the Smart Antenna Research Group, Stanford University, Stanford, CA, USA, as a Visiting Professor. In 2007, he joined the Department of Electrical Engineering, Princeton University, Princeton, NJ, USA, as a Visiting Professor. From 2006 to 2011, he was the Head of the Institute of Communication Technology, Leibniz University of Hannover, Hannover, Germany. He is currently the Head of the Institute of Digital Signal Processing, University of Duisburg–Essen. He is also the Founder and a CEO of ID4us GmbH, Duisburg, an RFID Centric Company. He has authored or coauthored more than 300 papers in international journals and conference proceedings and *Ultra Wideband Systems with MIMO* (Wiley, 2010) and *Digital Signal Processing for RFID* (Wiley, 2015).

Dr. Kaiser was the General Chair of the IEEE International Conference on UltraWideBand, in 2008, the International Conference on Cognitive Radio Oriented Wireless Networks and Communications, in 2009, the IEEE Workshop on Cellular Cognitive Systems, in 2014, and the IEEE International Workshop on Mobile THz Systems (IWMTS) in the years 2018 and 2019. He was the Founding Editor-in-Chief of the *e-letter* of the IEEE Signal Processing Society. He is the Speaker of the Collaborative Research Center Mobile Material Characterization and Localization by Electromagnetic Sensing.

DOI: 10.1109/ACCESS.2019.2933427
URN: urn:nbn:de:hbz:464-20191030-145627-2